NPS-MA-02-001

NAVAL POSTGRADUATE SCHOOL
Monterey, California

High-Order Higdon Non-Reflecting Boundary Conditions for the Shallow Water Equations

by

Dan Givoli
Beny Neta

April 2002

Approved for public release; distribution is unlimited.
Prepared for: Naval Postgraduate School

20020520 215

NAVAL POSTGRADUATE SCHOOL
Monterey, California 93943-5000

RADM David R. Ellison
Superintendent

R. Elster
Provost

This report was prepared for Naval Postgraduate School and funded in part by Office of Naval Research.

This report was prepared by:

Dan Givoli
National Research Council
Senior Research Associate

Beny Neta
Professor
Mathematics Department

Reviewed by:

Michael A. Morgan, Chair
Mathematics Department

Released by:

D. W. Netzer
Associate Provost and
Dean of Research

REPORT DOCUMENTATION PAGE

Form approved

OMB No 0704-0188

Public reporting burden for this collection of information is estimated to average 1 hour per response, including the time for reviewing instructions, searching existing data sources, gathering and maintaining the data needed, and completing and reviewing the collection of information. Send comments regarding this burden estimate or any other aspect of this collection of information, including suggestions for reducing this burden, to Washington Headquarters Services, Directorate for information Operations and Reports, 1215 Jefferson Davis Highway, Suite 1204, Arlington, VA 22202-4302, and to the Office of Management and Budget, Paperwork Reduction Project (0704-0188), Washington, DC 20503.

1. AGENCY USE ONLY (Leave blank)	2. REPORT DATE	3. REPORT TYPE AND DATES COVERED
	April 2002	1 August 2001 - 31 March 2002

4. TITLE AND SUBTITLE

High-Order Higdon Non-Reflecting Boundary Conditions for the Shallow Water Equations

5. FUNDING

N0001402WR20211

6. AUTHOR(S)

Dan Givoli and Beny Neta

7. PERFORMING ORGANIZATION NAME(S) AND ADDRESS(ES)

Naval Postgraduate School
Monterey, CA 93943

8. PERFORMING ORGANIZATION REPORT NUMBER

NPS-MA-02-001

9. SPONSORING/MONITORING AGENCY NAME(S) AND ADDRESS(ES)

Office of Naval Research
Marine Meteorology and Atmospheric Effects
800 North Quincy Street,
Ballston Tower One
Arlington, VA 22217-5660

10. SPONSORING/MONITORING AGENCY REPORT NUMBER

11. SUPPLEMENTARY NOTES

Approved for public release; distribution is unlimited.

12a. DISTRIBUTION/AVAILABILITY STATEMENT

12b. DISTRIBUTION CODE

13. ABSTRACT (Maximum 200 words.)

In this report we document the implementation of high order Higdon nonreflecting boundary conditions. We suggest a way to choose the parameters and demonstrate numerically the efficiency of our choice. The model we used is the shallow water equations and as a special case the Klein-Gordon equation. These equations are solved by the finite difference method. We comment on the use of finite elements and demonstrate a new, more efficient method. The case of curved boundary is discussed. We close with a list of topics for research.

14. SUBJECT TERMS

Lateral boundary conditions, High order, Finite differences

15. NUMBER OF PAGES

26

16. PRICE CODE

17. SECURITY CLASSIFICATION OF REPORT	18. SECURITY CLASSIFICATION OF THIS PAGE	19. SECURITY CLASSIFICATION OF ABSTRACT	20. LIMITATION OF ABSTRACT
UNCLASSIFIED	UNCLASSIFIED	UNCLASSIFIED	

Abstract

In this report we document the implementation of high order Higdon nonreflecting boundary conditions. We suggest a way to choose the parameters and demonstrate numerically the efficiency of our choice. The model we used is the shallow water equations and as a special case the Klein-Gordon equation. These equations are solved by the finite difference method. We comment on the use of finite elements and demonstrate a new, more efficient method. The case of curved boundary is discussed. We close with a list of topics for research.

1. Statement of the Problem

Consider the shallow water equations (SWEs) in a semi-infinite channel. For simplicity we assume that the channel has a flat bottom and that there is no advection, although these assumptions may be removed in future studies. We do take into account rotation (Coriolis) effects. A Cartesian coordinate system (x, y) is introduced such that the channel is parallel to the x direction, as shown in the figure. The width of the channel is denoted b.

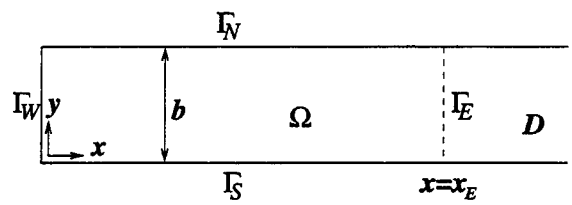

Figure 1: Setup for the wave-guide problem in a semi-infinite wave guide

The SWEs are (see [1]):

$$\partial_t u + \mu u \partial_x u + \mu v \partial_y u - f v = -g\ \partial_x \eta\ , \tag{1}$$

$$\partial_t v + \mu u \partial_x v + \mu v \partial_y v + f u = -g\ \partial_y \eta\ , \tag{2}$$

$$\partial_t \eta + \mu u \partial_x \eta + \mu v \partial_y \eta + (h_0 + \mu \eta)\ (\partial_x u + \partial_y v) = 0\ . \tag{3}$$

Here t is time, $u(x, y, t)$ and $v(x, y, t)$ are the unknown velocities in the x and y directions, h_0 is the given water layer thickness (in the direction normal to the xy plane), $\eta(x, y, t)$ is the unknown water elevation above h_0, f is the Coriolis parameter, and g is the gravity acceleration. We use the following shorthand for partial derivatives

$$\partial_a^i = \frac{\partial^i}{\partial a^i}$$

The parameter μ is 1 for the nonlinear SWEs, and is 0 for the linearized SWEs with vanishing mean flow. We shall consider the latter as a special case in the sequel.

It can be shown (see [2]) that *a single* boundary condition must be imposed along the entire boundary to obtain a well-posed problem. On the south and north channel walls Γ_S and Γ_N we have $v = 0$ (no normal flow). On the west boundary Γ_W we prescribe η using the Dirichlet condition $\eta(0, y, t) = \eta_W(y, t)$, where $\eta_W(y, t)$ is a given function (incoming wave). At $x \to \infty$ the solution is known to be bounded and not to include any incoming waves. To complete the statement of the problem, initial values for u, v and η are given at time $t = 0$ in the entire domain.

We now truncate the semi-infinite domain by introducing an artificial east boundary Γ_E, located at $x = x_E$ (see figure). To obtain a well-posed problem in the finite domain Ω we need a single boundary condition on Γ_E. This should be a Non-Reflecting Boundary Condition (NRBC). We shall apply a high-order NRBC for the variable η. A discussion on this NRBC follows.

2. Higdon's NRBCs

On the artificial boundary Γ_E we use one of the *Higdon NRBCs* [3]. These NRBCs were presented and analyzed in a sequence of papers [4]–[8] for non-dispersive acoustic and elastic waves, and were extended in [3] for dispersive waves. Their main advantages are as follows:

1. The Higdon NRBCs are very *general*, namely they apply to a variety of wave problems, in one, two and three dimensions and in various configurations.
2. They form a *sequence* of NRBCs of increasing order. This enables one, in principle (leaving implementational issues aside for the moment), to obtain solutions with unlimited accuracy.
3. The Higdon NRBCs can be used, without any difficulty, for *dispersive* wave problems and for problems with layers. Most other available NRBCs are either designed for non-dispersive media (as in acoustics and electromagnetics) or are of low order (as in meteorology and oceanography).
4. For certain choices of the parameters, the Higdon NRBCs are equivalent to NRBCs that are derived from rational approximation of the dispersion relation (the Engquist-Majda conditions being the most well-known example). This has been proved by Higdon in [3] and in earlier papers. Thus, the Higdon NRBCs can be viewed as generalization of rational-approximation NRBCs.

The scheme developed here is different than the original Higdon scheme [3] in the following ways:

1. The discrete Higdon conditions were developed in the literature up to third order only, because of their algebraic complexity which increases rapidly with the order. Here we show how to easily implement these conditions to an *arbitrarily high order*. The scheme is coded once and for all for any order; the order of the scheme is simply an input parameter.
2. The original Higdon conditions were applied to the Klein-Gordon linear wave equation and to the elastic equations. Here we show how to apply them to the

SWEs (1)–(3).

3. The Higdon NRBCs involve some parameters which must be chosen. Higdon [3] discusses some general guidelines for their manual a-priori choice by the user. We shall show how these parameters can be chosen *automatically.* They may either be constant, or may change adaptively during the solution process.
4. We shall show how to improve the discretization of the Higdon NRBCs using higher-order Finite Difference stencils.
5. We shall show how the Higdon NRBCs may be incorporated in a *Finite Element* scheme.
6. (**Future.**) We shall extend these ideas to other configurations (full-space exterior problems in 2D and 3D, 3D wave guides, etc.).
7. (**Future.**) We shall try to extend these ideas to curved boundaries.

The Higdon NRBC of order J is

$$H_J : \qquad \left[\prod_{j=1}^{J} (\partial_t + C_j \partial_x)\right] \eta = 0 \quad \text{on} \quad \Gamma_E \ . \tag{4}$$

Here, the C_j are parameters which have to be chosen and which signify phase speeds in the x-direction. The boundary condition (4) is exact for all waves that propagate with an x-direction phase speed equal to either of $C_1, \ldots, C_J$. This is easy to see from the following consideration.

Consider a wave which satisfies the linearized SWEs (eqs. (1)–(3) with $\mu = 0$; see, e.g., Pedlosky [1], p. 77). It has the form

$$\eta = \eta_0 Y(y) \cos(kx - \omega t + \psi) \ , \tag{5}$$

where

$$\omega^2 = \begin{cases} C_0^2(k^2 + \frac{n^2\pi^2}{b^2}) + f^2 & ; n = 1, 2, \ldots \\ C_0^2 k^2 & ; n = 0 \end{cases} , \tag{6}$$

$$Y(y) = \begin{cases} \cos \dfrac{n\pi y}{b} - \dfrac{bf}{n\pi C_x} \sin \dfrac{n\pi y}{b} & ; n = 1, 2, \ldots \\ \exp(-fy/C_0) & ; n = 0 \end{cases} , \tag{7}$$

$$C_0 = \sqrt{h_0 g} \ , \tag{8}$$

$$C_x = \frac{\omega}{k} \ . \tag{9}$$

In (5)–(9), η_0 is the wave amplitude, ψ is its phase, k is the x-component wave number, ω is the wave frequency, C_0 is the reference wave speed (which is both the phase speed and the group speed for the non-dispersive case $f = 0$), and C_x is the x-direction phase velocity. Eq. (6) is the dispersion relation. The solutions corresponding to the modes $n = 1, 2, \ldots$ are Poincaré waves, whereas the solution corresponding to $n = 0$ is

the Kelvin wave. These complete the set of all wave solutions for wave number k and mode n. There are also solutions that decay exponentially in the x direction. However, Higdon's NRBCs ignore them. They are usually not of great concern, since the decaying modes are expected to be insignificant at Γ_E, provided that Γ_E is sufficiently far away from where the waves are generated.

Now, it is easy to verify that if one of the C_j's in (4) is equal to C_x, then the wave (5) satisfies the boundary condition (4) exactly.

We make a few observations:

- From (6) and (9) we have

$$C_x = \begin{cases} \sqrt{C_0^2 + \dfrac{C_0^2 n^2 \pi^2 / b^2 + f^2}{k^2}} & ; n = 1, 2, \ldots \\ C_0 & ; n = 0 \end{cases} . \tag{10}$$

  Thus, always $C_x \geq C_0$; hence one should take $C_j \geq C_0$. In general, the solution consists of an infinite number of waves of the form (5) with different phase speeds.

- The first-order condition H_1 is a Sommerfeld-like boundary condition. If we set $C_1 = C_0$ we get the classical Sommerfeld-like NRBC. A lot of work in the meteorological literature is based on using H_1 with a specially chosen C_1. Pearson [9] used a special but constant value of C_1, while in the scheme devised by Orlanski [10] and in later improved schemes [11]–[14] the C_1 changes dynamically and locally in each time-step based on the solution from the previous time-step. Some of the limited-area weather prediction codes used today are based on such schemes, e.g., COAMPS [15]. See also the recent papers [16]–[18] where several such schemes are compared.

- The condition H_J involves up to Jth-order normal and temporal derivatives. In fact, it has the form

$$\sum_{j=0}^{J} A_j \, \partial_x^j \partial_t^{J-j} \eta = 0 \, , \tag{11}$$

  which is obtained by expanding (4).

- It is easy to show (see Higdon [3] for a similar setting) that when a wave of the form (5) impinges on the boundary Γ_E where the NRBC H_J is imposed, the resulting *reflection coefficient* is

$$R = \prod_{j=1}^{J} \left| \frac{C_j - C_x}{C_j + C_x} \right| . \tag{12}$$

  Again we see that if $C_j = C_x$ for one of the j's then $R = 0$, namely there is no reflection and the NRBC is exact. Moreover, we see that the reflection coefficient is a product of J factors, *each of which is smaller than 1.* This implies that the reflection coefficient becomes smaller as the order J increases regardless of the choice made for the parameters C_j. Of course, a good choice for the C_j would lead to better accuracy with a lower order J, but even if we miss the correct C_j's

considerably (say, if we make the simplest choice $C_j = C_0$ for $j = 1, \ldots, J$), we are still guaranteed to reduce the spurious reflection as we increase the order J. This is an important property of the Higdon's NRBCs and is the reason for their robustness.

- In [6], Higdon points to the possibility of a long-time instability that might occur when one uses a NRBC with high-order derivatives. If the interior governing equations and the NRBC both admit solutions at zero wave number and frequency, and if the data in the problem include such "zero modes," then a slowly-growing smooth instability is possible. Whether this shows up in practice depends on the order of the derivatives in the NRBC and the number of spatial dimensions. However, these difficulties do not arise in the presence of dispersion, or if the data are confined to nontrivial modes.

3. Discretization of Higdon's NRBCs

The Higdon condition H_J is a product of J operators of the form $\partial_t + C_j \partial_x$. Consider the following Finite Difference (FD) approximations:

$$\partial_t \simeq \frac{I - S_t^-}{\Delta t} \quad , \quad \partial_x \simeq \frac{I - S_x^-}{\Delta x} \; . \tag{13}$$

In (13), Δt and Δx are, respectively, the time-step size and grid spacing in the x direction, I is the identity operator, and S_t^- and S_x^- are shift operators defined by

$$S_t^- \eta_{pq}^n = \eta_{pq}^{n-1} \quad , \quad S_x^- \eta_{pq}^n = \eta_{p-1,q}^n \; . \tag{14}$$

Here and elsewhere, η_{pq}^n is the FD approximation of $\eta(x, y, t)$ at grid point (x_p, y_q) and at time t_n. We use (13) in (4) to obtain:

$$\left[\prod_{j=1}^{J} \left(\frac{I - S_t^-}{\Delta t} + C_j \frac{I - S_x^-}{\Delta x} \right) \right] \eta_{Eq}^n = 0 \; . \tag{15}$$

Here, the index E correspond to a grid point on the boundary Γ_E. Higdon has solved this difference equation (and also a slightly more involved equation that is based on time- and space-averaging approximations for ∂_x and ∂_t; see next section) for $J \leq 3$ to obtain an explicit formula for η_{Eq}^n. This formula is used to find the current values on the boundary Γ_E *after* the solution in the interior points and on the other boundaries has been updated. The formula for $J = 2$ is found in [8], and the one for $J = 3$ appears in the appendix of [7]. The algebraic complexity of these formulas increases rapidly with the order J. It is thus not surprising that we have not found in the literature any report on the implementation of the Higdon NRBCs beyond $J = 3$.

Now we show how to implement the Higdon NRBCs *to any order* using a simple algorithm. To this end, we first multiply (15) by Δt and rearrange to obtain

$$Z \equiv \left[\prod_{j=1}^{J} \left(a_j I + d_j S_t^- + e_j S_x^- \right) \right] \eta_{Eq}^n = 0 \; , \tag{16}$$

where

$$a_j = 1 + \frac{C_j \Delta t}{\Delta x} , \tag{17}$$

$$d_j = -1 , \tag{18}$$

$$e_j = -\frac{C_j \Delta t}{\Delta x} . \tag{19}$$

The coefficient d_j actually does not depend on j, but we keep this notation to allow easy extensions to the scheme (see later). Now, Z in (16) can be written as a sum of 3^J terms, each one is an operator acting on η^n_{Eq}, namely

$$Z \equiv \sum_{m=0}^{3^J-1} A_m P_m \eta^n_{Eq} = 0 . \tag{20}$$

Here A_m is a coefficient depending on the a_j, d_j and e_j, and P_m is an operator involving products of I, S_t^- and S_x^-. All the terms in the sum in (20) are computable at the current time step n, except the one which involves only the identity operator and no shift operators. If we let this term correspond to $m = 0$, then $P_0 = I$ and

$$A_0 = \prod_{j=1}^{J} a_j . \tag{21}$$

Thus we get from (20)

$$Z \equiv A_0 \eta^n_{Eq} + Z^* = 0 , \tag{22}$$

where

$$Z^* = \sum_{m=1}^{3^J-1} A_m P_m \eta^n_{Eq} . \tag{23}$$

From (22) we get

$$\eta^n_{Eq} = -Z^*/A_0 , \tag{24}$$

which is the desired value of η on the boundary Γ_E.

The problem now reduces to calculating Z^* given by (23). We do this using the algorithm described in Box 1.

Note that we need to store $\eta^{\hat{n}}_{\hat{i}q}$ values for $\hat{i} = E, E-1, \ldots, E-J$ and $\hat{n} = n, n-1, \ldots, n-J$. In other words, we have to store the history of the values of η for a layer of thickness $J+1$ points near the boundary Γ_E and for $J+1$ time levels (including the current one). If there are N_y grid points in the y direction, then the amount of storage needed in a simple storage scheme is $(J+1)^2 N_y$. However, one can save in storage by exploiting the fact that not all values $\eta^{\hat{n}}_{\hat{i}q}$ are needed, but only those for which $(E-\hat{i}) + (n-\hat{n}) \leq J$. This is clear from (11) and also from (16). For example, the solution at time t_{n-J} should be stored only for points on the boundary Γ_E itself.

- Start with $Z^* = 0$. Calculate $A_0 = \prod_{j=1}^{J} a_j$.
- Loop over the integers $m = 1, \ldots, 3^J - 1$.
  - For a given m, transform m into a number r in base 3, consisting of the digits 0, 1 and 2 only. The length of r will be at most J digits. Store the J digits of r in the vector $D_r(j)$, $j = 1, \ldots, J$.
    Example: Suppose that $J = 6$ and $m = 227$. Since 227 in base 3 is $r = 22102$, we will get $D_r = \{\ 0\ 2\ 2\ 1\ 0\ 2\ \}$.
  - Use D_r to calculate the coefficient A_m. To this end, start with $A_m = 1$, loop over $j = 1, \ldots, J$, and for each j multiply A_m by the factor a_j (if $D_r(j) = 0$) or d_j (if $D_r(j) = 1$) or e_j (if $D_r(j) = 2$).
    Example: For $J = 6$ and $m = 227$, we have received the vector D_r above. Then $A_{227} = a_1 e_2 e_3 d_4 a_5 e_6$.
  - Use D_r to calculate the operator action $P_m \eta_{Eq}^n$. To this end, start with $\hat{n} = n$ and $\hat{i} = E$, loop over $j = 1, \ldots, J$, and for each j subtract 1 from $\hat{n}$ (if $D_r(j) = 1$) or subtract 1 from $\hat{i}$ (if $D_r(j) = 2$) or do nothing (if $D_r(j) = 0$). After the loop ends we have $P_m \eta_{Eq}^n = \eta_{\hat{i}q}^{\hat{n}}$.
    Example: For the case $J = 6$ and $m = 227$ considered above, we get $\hat{n} = n - 1$ (because the digit "1" appears only once in D_r), and $\hat{i} = E - 3$ (because the digit "2" appears three times in D_r). Hence $P_{227} \eta_{Eq}^n = \eta_{E-3,q}^{n-1}$.
  - Update: $Z^* \leftarrow Z^* + A_m \eta_{\hat{i}q}^{\hat{n}}$.
- Next m.
- $\eta_{Eq}^n = -Z^*/A_0$.

Box 1. Algorithm for implementing the Higdon NRBC of order J, using high-order FD discretization.

4. Improved Discrete Higdon NRBCs

The discretization scheme described in the previous section is based on the FD approximations given by (13). These approximations can be improved in several ways. For example:

(a) We can take

$$\partial_t \simeq \frac{I - S_t^-}{\Delta t}\left((1-b)I + bS_x^-\right) \quad , \quad \partial_x \simeq \frac{I - S_x^-}{\Delta x}\left((1-b)I + bS_t^-\right) \ , \tag{25}$$

where $0 \leq b \leq 1$. Thus, the temporal difference is calculated with a weighted average in space while the spatial difference is calculated with a weighted averaged in time. The formulas (13) correspond to $b = 0$. In [3], Higdon has used this approximation with $b = 0.5$, and reported a slight improvement in the results compared to the use of (13).

(b) We can take one-sided approximations for the x- and t-derivatives [19], i.e.,

$$\partial_t \simeq \frac{3I - 4S_t^- + (S_t^-)^2}{2\Delta t} \quad , \quad \partial_x \simeq \frac{3I - 4S_x^- + (S_x^-)^2}{2\Delta x} \ . \tag{26}$$

These approximations are second-order accurate, as opposed to those in (13) which are first-order accurate.

(c) We can combine the two types of approximations given above, namely

$$\partial_t \simeq \frac{3I - 4S_t^- + (S_t^-)^2}{2\Delta t}\left((1-b)I + bS_x^-\right) \ , \tag{27}$$

$$\partial_x \simeq \frac{3I - 4S_x^- + (S_x^-)^2}{2\Delta x}\left((1-b)I + bS_t^-\right) \ . \tag{28}$$

The procedure described in the previous section (see Box 1) for implementing the Higdon NRBCs can easily be modified to admit these improved approximations. The main feature that has to be changed in the algorithm outlined in Box 1 is the *base* to which the counting decimal integer m is transformed. For example, consider the approximation (a) above replacing (13). In this case (16), which involves three basic operators (I, S_t^- and S_x^-) is replaced by

$$Z \equiv \left[\prod_{j=1}^{J}\left(a_j I + d_j S_t^- + e_j S_x^- + g_j S_t^- S_x^-\right)\right]\eta_{Eq}^n = 0 \ , \tag{29}$$

which involves *four* basic operators (I, S_t^-, S_x^- and $S_t^- S_x^-$). Therefore, the counter m in the main loop in Box 1 will range from 1 to $4^J - 1$, and all the calculation will be performed in base 4 rather than in base 3. Similarly, the approximations (b) and (c) will require calculations in base 5 and base 8, respectively. The alternations needed in the coding are minor, but naturally the computational time associated with these improved approximations would increase dramatically.

We note that when one uses a high-order NRBC (namely H_J with a large J), the discrete operator involved is of high-order even when the simplest formulas in (13) are used to approximate the x- and t-derivatives. Thus, the importance of the improvements discussed above diminishes when J increases. In fact, there is a point in incorporating such improvements in the scheme only if a low-order condition (say, $J \leq 3$) is employed.

5. The Interior Scheme

We consider explicit FD interior discretization schemes for the SWEs (1)–(3) to be used in conjunction with the H_J condition. The interaction between the H_J condition and the interior scheme is of concern, since simple choices for an explicit interior scheme turn out to give rise to long-time instabilities. We have tried the Miller-Pearce time-integration [20], Leap-Frog [21], a version of semi-implicit time-integration [22] and the MacCormack scheme [21, 23] (which is equivalent for linear problems to the Lax-Wendroff scheme). They are all stable for a sufficiently small time step when used with the boundary condition H_1 (which is a Sommerfeld-like condition as previously mentioned), but they all become unstable for $J \geq 2$. The instability appears earlier in time when J becomes larger.

Higdon [3] has proved, in the context of the scalar Klein-Gordon equation,

$$\partial_t^2 \eta - C_0^2 \nabla^2 \eta + f^2 \eta = 0 \ , \tag{30}$$

that the discrete NRBCs (15) are stable if the interior scheme is the standard *second-order centered* difference scheme

$$\begin{aligned} \eta_{pq}^{n+1} = 2\eta_{pq}^n - \eta_{pq}^{n-1} &+ \left(\frac{C_0 \Delta t}{\Delta x}\right)^2 \left(\eta_{p+1,q}^n - 2\eta_{p,q}^n + \eta_{p-1,q}^n\right) \\ &+ \left(\frac{C_0 \Delta t}{\Delta y}\right)^2 \left(\eta_{p,q+1}^n - 2\eta_{p,q}^n + \eta_{p,q-1}^n\right) - (f\Delta t)^2 \eta_{p,q}^n \ . \end{aligned} \tag{31}$$

Now we shall show how the SWEs (1)–(3) can be discretized in such a way as to mimic (31) and to lead to a stable scheme.

First we define the new variables

$$V^+ = h_0(\partial_x u + \partial_y v) \quad , \quad V^- = h_0(\partial_x v - \partial_y u) \ . \tag{32}$$

From the SWEs (1)–(3) we obtain equations which involve these two variables. By differentiating (1) and (2) with respect to x and to y, respectively, and then summing the results, we get the equation

$$\partial_t V^+ - f V^- + g h_0 \nabla^2 \eta = N_1 \ , \tag{33}$$

where

$$N_1 = \mu h_0 \ [\partial_x(u\partial_x u) + \partial_x(v\partial_y u) + \partial_y(u\partial_x v) + \partial_y(v\partial_y v)] \ . \tag{34}$$

Note that N_1 is the nonlinear part of eq. (33). Similarly, we differentiate (2) and (1) with respect to x and to y, respectively, and then subtract the second from the first to obtain

$$\partial_t V^- + f V^+ = N_2 \ , \tag{35}$$

where

$$N_2 = \mu h_0 \ [\partial_x(u\partial_x v) + \partial_x(v\partial_y v) - \partial_y(u\partial_x u) - \partial_y(v\partial_y u)] \ . \tag{36}$$

We write (3) as

$$\partial_t \eta + V^+ = N_3 \ , \tag{37}$$

where

$$N_3 = \mu \, [\partial_x(u\eta) + \partial_y(v\eta)] \ . \tag{38}$$

Finally we also consider the time derivative of eq. (37), namely

$$\partial_{tt}\eta + \partial_t V^+ = \partial_t N_3 \ . \tag{39}$$

Now we base the interior scheme on eqs. (33), (35), (37) and (39). First, we discretize (37) to obtain an updating formula for V^+:

$$(V^+)_{pq}^{n+1} = N_3^n - \frac{\eta_{pq}^n - \eta_{pq}^{n-1}}{\Delta t} \ . \tag{40}$$

The notation N_3^n means that we calculate all the variables appearing in the expression for N_3 at time-step n. We shall discuss the discretization of the spatial derivatives in N_3 later. Then we use (35) to update $V_t^- \equiv \partial_t V^-$:

$$(V_t^-)_{pq}^{n+1} = N_2^n - f(V^+)_{pq}^{n+1} \ . \tag{41}$$

Next we integrate (41) to update V^-:

$$(V^-)_{pq}^{n+1} = (V^-)_{pq}^n + \Delta t (V_t^-)_{pq}^{n+1} \ . \tag{42}$$

Now we use (33) to update $V_t^+ \equiv \partial_t V^+$. We use second-order central differences in space to approximate $\nabla^2\eta$:

$$(V_t^+)_{pq}^{n+1} = N_1^n + f(V^-)_{pq}^{n+1} - g h_0 \left(\frac{\eta_{p+1,q}^n - 2\eta_{p,q}^n + \eta_{p-1,q}^n}{\Delta x^2} + \frac{\eta_{p,q+1}^n - 2\eta_{p,q}^n + \eta_{p,q-1}^n}{\Delta y^2} \right) \ . \tag{43}$$

Finally we use eq. (39) to update η. We use second-order central differences in time to approximate $\partial_{tt}\eta$:

$$\eta_{pq}^{n+1} = 2\eta_{pq}^n - \eta_{pq}^{n-1} - \Delta t^2 (V_t^+)_{pq}^{n+1} + \Delta t (N_3^n - N_3^{n-1}) \ . \tag{44}$$

After η_{pq}^{n+1} is known, the updated values for u and v, i.e., u_{pq}^{n+1} and v_{pq}^{n+1} may be found in a number of ways. We have chosen to integrate the original SWEs (1) and (2) using a forward FD approximation in time to obtain these values.

It is easy to show that in the linear case, and with zero initial conditions, the updating formula for η, eq. (44), coincides with the formula (31) for the Klein-Gordon

equation. Indeed, in this case $(V^-)^{n+1} = f\eta^n$, and using (40)–(44) without the nonlinear terms leads exactly to formula (31). Thus stability is guaranteed in this case.

In the nonlinear case, we have to calculate the quantities N_1^n, N_2^n and N_3^n. These involve first- and second-order spatial derivatives. All these derivatives may be calculated using second-order centered differences.

(**Future:** Find other "more natural" schemes that are stable with H_J.)

6. An Alternative Formulation With Auxiliary Functions

Now we show how to rewrite the Higdon boundary conditions *with no high-order derivatives*, by the use of auxiliary variables. This form of boundary condition has the advantages that after discretization it involves only degrees of freedom on the boundary Γ_E itself, that no high-order discrete schemes are needed, and that the history of the solution does not have to be stored. As a result, it is more amenable, compared to the previous formulation, for incorporation in a Finite Element scheme. For simplicity, we consider the linear Klein-Gordon equation (dispersive wave equation)

$$\partial_t^2\eta - C_0^2\nabla^2\eta + f^2\eta = 0 \ , \tag{45}$$

rather than the SWEs. We assume that C_0 and f do not depend on x (the direction normal to the artificial boundary Γ_E) or on t, but they may be functions of y (the direction tangent to Γ_E).

We first replace the Higdon condition (4) by the equivalent condition

$$H_J : \qquad \left[\prod_{j=1}^{J}\left(\partial_x + \frac{1}{C_j}\partial_t\right)\right]\eta = 0 \quad \text{on} \quad \Gamma_E \ . \tag{46}$$

Now we introduce the auxiliary functions $\phi_1, \ldots, \phi_{J-1}$, which are defined on Γ_E as well as in the exterior domain outside Γ_E (namely the domain $x > x_E$), denoted D. (Eventually we shall use these functions only on Γ_E, but the derivation requires that they be defined in D as well, or at least in a non-vanishing region adjacent to Γ_E.) The functions ϕ_j are defined via the relations

$$\left(\partial_x + \frac{1}{C_1}\partial_t\right)\eta = \phi_1 \ , \tag{47}$$

$$\left(\partial_x + \frac{1}{C_2}\partial_t\right)\phi_1 = \phi_2 \ , \tag{48}$$

$$\vdots$$

$$\left(\partial_x + \frac{1}{C_J}\partial_t\right)\phi_{J-1} = 0 \ . \tag{49}$$

By definition, these relations hold in D, and also on Γ_E. It is easy to see that (47)–(49), when imposed as boundary conditions on Γ_E, are equivalent to the single boundary condition (46). If we also define

$$\phi_0 \equiv \eta \quad , \quad \phi_J \equiv 0 \, , \tag{50}$$

then we can write (47)–(49) concisely as

$$\left(\partial_x + \frac{1}{C_j}\partial_t\right)\phi_{j-1} = \phi_j \quad , \quad j = 1, \ldots, J \, . \tag{51}$$

This set of conditions involves only first-order derivatives. However, due to the appearance of the x-derivative in (51), one cannot discretize the ϕ_j on the boundary Γ_E alone. Therefore we shall manipulate (51) in order to get rid of the x-derivative.

The function η satisfies the wave equation (45) in D. The function ϕ_1 is obtained by applying a linear operator to η, as in (47); hence it is clear that ϕ_1 also satisfies the same equation in D. Similarly, we deduce that each of the functions ϕ_j satisfies a wave equation like (45). (Here we needed the assumption that C_0 and f do not depend on x or on t.) Namely,

$$\partial_x^2\phi_j + \partial_y^2\phi_j - \frac{1}{C_0^2}\partial_t^2\phi_j - \frac{f^2}{C_0^2}\phi_j = 0 \, . \tag{52}$$

Now, we make use of the following identity:

$$\partial_x^2\phi_j = \left(\partial_x - \frac{1}{C_{j+1}}\partial_t\right)\left(\partial_x + \frac{1}{C_{j+1}}\partial_t\right)\phi_j + \frac{1}{C_{j+1}^2}\partial_t^2\phi_j \, . \tag{53}$$

Substituting (53) in (52) and replacing j with $j-1$ everywhere yields, for $j = 1, \ldots, J$,

$$\left(\partial_x - \frac{1}{C_j}\partial_t\right)\left(\partial_x + \frac{1}{C_j}\partial_t\right)\phi_{j-1} + \left(\frac{1}{C_j^2} - \frac{1}{C_0^2}\right)\partial_t^2\phi_{j-1} + \partial_y^2\phi_{j-1} - \frac{f^2}{C_0^2}\phi_{j-1} = 0 \, . \tag{54}$$

From this and (51) we get, for $j = 1, \ldots, J$,

$$\left(\partial_x - \frac{1}{C_j}\partial_t\right)\phi_j + \left(\frac{1}{C_j^2} - \frac{1}{C_0^2}\right)\partial_t^2\phi_{j-1} + \partial_y^2\phi_{j-1} - \frac{f^2}{C_0^2}\phi_{j-1} = 0 \, . \tag{55}$$

On the other hand, (51) can also be written as

$$\left(\partial_x + \frac{1}{C_{j+1}}\partial_t\right)\phi_j = \phi_{j+1} \, , \quad j = 0, \ldots, J-1 \, . \tag{56}$$

We subtract (55) from (56) to finally obtain, for $j = 1, \ldots, J-1$,

$$\left(\frac{1}{C_j} + \frac{1}{C_{j+1}}\right)\partial_t\phi_j = \phi_{j+1} + \left(\frac{1}{C_j^2} - \frac{1}{C_0^2}\right)\partial_t^2\phi_{j-1} + \partial_y^2\phi_{j-1} - \frac{f^2}{C_0^2}\phi_{j-1} \, . \tag{57}$$

The boundary condition (57) does not involve x-derivatives, as desired. In addition, there are no high y- and t-derivatives in (57) beyond second order.

Rewriting (47), (50) and (57), we can summarize this formulation of the Higdon Jth-order NRBC on Γ_E as follows:

$$\beta_0 \partial_t \eta + \partial_x \eta = \phi_1 \ , \tag{58}$$

$$\beta_j \partial_t \phi_j - \alpha_j \partial_t^2 \phi_{j-1} - \partial_y^2 \phi_{j-1} + \lambda \phi_{j-1} = \phi_{j+1} \quad , \quad j = 1, \ldots, J-1 \ , \tag{59}$$

$$\alpha_j = \frac{1}{C_j^2} - \frac{1}{C_0^2} \quad , \quad \beta_0 = \frac{1}{C_1} \quad , \quad \beta_j = \frac{1}{C_j} + \frac{1}{C_{j+1}} \quad , \quad \lambda = \frac{f^2}{C_0^2} \ , \tag{60}$$

$$\phi_0 \equiv \eta \quad , \quad \phi_J \equiv 0 \ . \tag{61}$$

Future: Implement using FD approximation and check various interior schemes with this formulation. Maybe interior schemes that are unstable with the discrete BC of Section 3 become stable with the discrete BC of this section.

7. Finite Element Formulation

Now we show how the Higdon boundary condition in the form (58)–(61) can be incorporated in a Finite Element (FE) formulation.

Again we consider the linear Klein-Gordon equation

$$\partial_t^2 \eta - C_0^2 \nabla^2 \eta + f^2 \eta = 0 \ . \tag{62}$$

If on the artificial boundary Γ_E the homogeneous Neumann condition $\partial_x \eta = 0$ was applied, the resulting semi-discrete system of ODEs would have been the standard one, namely

$$\boldsymbol{M}\ddot{\boldsymbol{d}} + \boldsymbol{K}\boldsymbol{d} = \boldsymbol{F} \ . \tag{63}$$

Here $\boldsymbol{M}$, $\boldsymbol{K}$ and $\boldsymbol{F}$, are, respectively, the global mass matrix, stiffness matrix, and load vector, and a superposed dot indicated differentiation with respect to time. The dimension of all the global arrays in (63) is N, the total number of degrees of freedom. On the element level, the element mass and stiffness matrices, which contribute to $\boldsymbol{M}$ and $\boldsymbol{K}$ via the assembly operation, are given by

$$m_{ab}^e = \int_{\Omega^e} N_a N_b \, d\Omega \ , \tag{64}$$

$$k_{ab}^e = \int_{\Omega^e} (C_0^2 \, \boldsymbol{\nabla} N_a \cdot \boldsymbol{\nabla} N_b + f^2 N_a N_b) \, d\Omega \ . \tag{65}$$

Here Ω^e is the element domain, and N_a is the FE shape function corresponding to node a of the element (for an η degree of freedom). The load vector $\boldsymbol{F}$ in (63) includes information related to the boundary condition given on the boundary Γ_W.

When the boundary condition (58), namely,

$$-\partial_x \eta = \beta_0 \partial_t \eta - \phi_1 \quad \text{on} \quad \Gamma_E \ , \tag{66}$$

is incorporated in the FE formulation, (63) becomes

$$\boldsymbol{M}\ddot{\boldsymbol{d}} + \boldsymbol{C}\dot{\boldsymbol{d}} + \boldsymbol{K}\boldsymbol{d} = \boldsymbol{F} + \boldsymbol{G}\boldsymbol{\phi}_1 \ . \tag{67}$$

Here $\boldsymbol{\phi}_1$ is the unknown vector whose entries are the nodal values of the variable ϕ_1 on Γ_E. $\boldsymbol{C}$ is an $N \times N$ damping matrix, and $\boldsymbol{G}$ is an $N \times N_E$ rectangular matrix, where N_E is the number of degrees of freedom on Γ_E. The element-level analogs of $\boldsymbol{C}$ and $\boldsymbol{G}$ are:

$$c^e_{ab} = \int_{\Gamma^e_E} \beta_0 C_0^2 N_a N_b \, d\Gamma \ , \tag{68}$$

$$g^e_{ab} = \int_{\Gamma^e_E} C_0^2 N_a N_b^{(1)} \, d\Gamma \ . \tag{69}$$

Here $\Gamma^e_E = \partial\Omega^e \cap \Gamma_E$, and $N_b^{(1)}$ is the FE shape function corresponding to node b for the degree of freedom associated with ϕ_1. Of course it is convenient to choose $N_b^{(1)} \equiv N_b$, but it remains to be checked that this combination leads to a stable scheme.

The jth boundary condition (59) leads to the following system of ODEs:

$$\boldsymbol{C}_j \dot{\boldsymbol{\phi}}_j = \boldsymbol{P}_j \ddot{\boldsymbol{\phi}}_{j-1} - \boldsymbol{Q}_j \boldsymbol{\phi}_{j-1} + \boldsymbol{R}_j \boldsymbol{\phi}_{j+1} \quad , \quad j = 1, \ldots, J-1 \ . \tag{70}$$

Here all the matrices are $N_E \times N_E$. The vector $\boldsymbol{\phi}_j$ is the unknown vector whose entries are the nodal values of the variable ϕ_j on Γ_E. Relating to (61), we have that $\boldsymbol{\phi}_J \equiv 0$, and that $\boldsymbol{\phi}_0$ is the N_E-dimensional vector whose entries are equal to the entries of the N-dimensional vector $\boldsymbol{d}$ for the degrees of freedom on Γ_E. The element matrices analogous to $\boldsymbol{C}_j$, $\boldsymbol{P}_j$, $\boldsymbol{Q}_j$ and $\boldsymbol{R}_j$ are:

$$(c^e_j)_{ab} = \int_{\Gamma^e_E} \beta_j N_a^{(j)} N_b^{(j)} \, d\Gamma \ , \tag{71}$$

$$(p^e_j)_{ab} = \int_{\Gamma^e_E} \alpha_j N_a^{(j)} N_b^{(j-1)} \, d\Gamma \ , \tag{72}$$

$$(q^e_j)_{ab} = \int_{\Gamma^e_E} N_a^{(j)\prime} N_b^{(j-1)\prime} + \lambda N_a^{(j)} N_b^{(j-1)} \, d\Gamma \ , \tag{73}$$

$$(r^e_j)_{ab} = \int_{\Gamma^e_E} N_a^{(j)} N_b^{(j+1)} \, d\Gamma \ . \tag{74}$$

Here $N_b^{(j)}$ is the FE shape function corresponding to node b for the degree of freedom associated with ϕ_j. Again, it is convenient to have equal $N_a^{(j)}$ for all the j's. In this case (and assuming constant coefficients in each element) the matrices in (68), (69), (71), (72) and (74) are all the same up to a constant factor. The primes in (73) indicate differentiation with respect to y; we have used integration by parts to obtain this symmetric expression.

Now we propose a time-integration scheme for the solution of (67) and (70), which constitute J coupled systems of ODEs. We discretize all these systems based on the Newmark [24] family of schemes for second-order ODEs in time (with parameters β and γ). Note that the system (70) is actually first-order in time for $\boldsymbol{\phi}_j$, so that the "mass matrix" is zero for this system. However, we can still use the Newmark method as long as the "damping matrix" $\boldsymbol{C}_j$ is non-singular, which is indeed the case. The advantage of using the Newmark scheme for (70) (as opposed, say, to using the generalized trapezoidal scheme) is that it yields the "acceleration," namely the second time-derivative

of ϕ_j, in each time-step. This "acceleration" is needed because it appears in the right side of (70) as $\ddot{\phi}_{j-1}$.

We denote the approximations of $\boldsymbol{d}$, $\dot{\boldsymbol{d}}$ and $\ddot{\boldsymbol{d}}$ at time-step n by $\boldsymbol{d}_n$, $\boldsymbol{v}_n$ and $\boldsymbol{a}_n$, respectively. We also denote the approximations of $\boldsymbol{\phi}_j$ and $\dot{\boldsymbol{\phi}}_j$ and $\ddot{\boldsymbol{\phi}}_j$ at time-step n by $\boldsymbol{U}_{j,n}$ $\boldsymbol{V}_{j,n}$ and $\boldsymbol{A}_{j,n}$, respectively.

In predictor-corrector form, the proposed time-integration scheme is:

Prediction:

$$\tilde{\boldsymbol{d}}_{n+1} = \boldsymbol{d}_n + \Delta t \boldsymbol{v}_n + \frac{\Delta t^2}{2}(1-2\beta)\boldsymbol{a}_n \tag{75}$$

$$\tilde{\boldsymbol{v}}_{n+1} = \boldsymbol{v}_n + (1-\gamma)\Delta t \boldsymbol{a}_n \tag{76}$$

$$\tilde{\boldsymbol{U}}_{j,n+1} = \boldsymbol{U}_{j,n} + \Delta t \boldsymbol{V}_{j,n} + \frac{\Delta t^2}{2}(1-2\beta)\boldsymbol{A}_{j,n} \quad , \quad j = 1,\ldots,J-1 \tag{77}$$

$$\tilde{\boldsymbol{V}}_{j,n+1} = \boldsymbol{V}_{j,n} + (1-\gamma)\Delta t \boldsymbol{A}_{j,n} \quad , \quad j = 1,\ldots,J-1 \tag{78}$$

Solution:

$$(\boldsymbol{M} + \gamma\Delta t \boldsymbol{C} + \beta\Delta t^2 \boldsymbol{K})\boldsymbol{a}_{n+1} = \boldsymbol{F}_{n+1} + \boldsymbol{G}\tilde{\boldsymbol{U}}_{1,n+1} - \boldsymbol{C}\tilde{\boldsymbol{v}}_{n+1} - \boldsymbol{K}\tilde{\boldsymbol{d}}_{n+1} \tag{79}$$

$$\gamma\Delta t \boldsymbol{C}_j \boldsymbol{A}_{j,n+1} = \boldsymbol{P}_j \boldsymbol{A}_{j-1,n+1} - \boldsymbol{Q}_j \boldsymbol{U}_{j-1,n+1} + \boldsymbol{R}_j \tilde{\boldsymbol{U}}_{j+1,n+1} - \boldsymbol{C}_j \tilde{\boldsymbol{V}}_{j,n+1} \quad , \quad j = 1,\ldots,J-1 \tag{80}$$

Correction:

$$\boldsymbol{d}_{n+1} = \tilde{\boldsymbol{d}}_{n+1} + \beta\Delta t^2 \boldsymbol{a}_{n+1} \tag{81}$$

$$\boldsymbol{v}_{n+1} = \tilde{\boldsymbol{v}}_{n+1} + \gamma\Delta t \boldsymbol{a}_{n+1} \tag{82}$$

$$\boldsymbol{U}_{j,n+1} = \tilde{\boldsymbol{U}}_{j,n+1} + \beta\Delta t^2 \boldsymbol{A}_{j,n+1} \quad , \quad j = 1,\ldots,J-1 \tag{83}$$

$$\boldsymbol{V}_{j,n+1} = \tilde{\boldsymbol{V}}_{j,n+1} + \gamma\Delta t \boldsymbol{A}_{j,n+1} \quad , \quad j = 1,\ldots,J-1 \tag{84}$$

Note the order in which these calculations should be done in each time step. First, the prediction phase is performed to yield $\tilde{\boldsymbol{d}}_{n+1}$ and $\tilde{\boldsymbol{v}}_{n+1}$, as well as $\tilde{\boldsymbol{U}}_{j,n+1}$ and $\tilde{\boldsymbol{V}}_{j,n+1}$ for all the j's. Then (79) is solved for $\boldsymbol{a}_{n+1}$. Then $\boldsymbol{d}_{n+1}$ and $\boldsymbol{v}_{n+1}$ are calculated in the Correction phase. Then (80) is solved with $j = 1$, for $\boldsymbol{A}_{1,n+1}$. Note that this solution involves $\boldsymbol{A}_{0,n+1}$ and $\boldsymbol{U}_{0,n+1}$, namely $\boldsymbol{a}_{n+1}$ and $\boldsymbol{d}_{n+1}$, which have already been computed. Then $\boldsymbol{U}_{1,n+1}$ and $\boldsymbol{V}_{1,n+1}$ are calculated in the Correction phase. Then (80) is solved with $j = 2$, for $\boldsymbol{A}_{2,n+1}$, using on the right side of (80) the vectors $\boldsymbol{A}_{1,n+1}$ and $\boldsymbol{U}_{1,n+1}$ which are already known. The procedure goes on in this fashion.

We have used the predicted vectors $\tilde{\boldsymbol{U}}_{j+1,n+1}$ in (79) and (80) rather than $\boldsymbol{U}_{j+1,n+1}$, since the latter is not known when solving for $\boldsymbol{a}_{n+1}$ or $\boldsymbol{A}_{j,n+1}$. However, it is possible to improve the accuracy (and stability?) of the process if a second cycle is performed after the $\boldsymbol{U}_{j,n+1}$ are calculated for all the j's. One can proceed "backwards," by solving (80) again for j ranging from $j = J-2$ to $j = 1$ and then also solving (79) again, while using in this second cycle the already computed vectors $\boldsymbol{U}_{j+1,n+1}$ instead of $\tilde{\boldsymbol{U}}_{j+1,n+1}$. Alternatively, one can start in the second cycle from (79) and proceed "forward" to solve the other equations, for $j = 1,\ldots,J-1$, one more time.

8. FD Discretization of the Auxiliary-Variable Formulation

In the previous section we showed how to discretize the NRBCs (58)–(61) by FEs. Now we show how to discretize them by FDs.

First we consider the boundary condition for η, (58). We discretize $\partial_x \eta$ on Γ_E by using the one-sided second-order approximation [19]

$$(\partial_x \eta)^n_{Eq} \simeq - \frac{-3\eta^n_{Eq} + 4\eta^n_{E-1,q} - \eta^n_{E-2,q}}{2\Delta x} . \tag{85}$$

From (58) we obtain a discrete formula for $\partial_t \eta$, i.e.,

$$(\partial_t \eta)^n_{Eq} \simeq \frac{1}{\beta_0} \left((\phi_1)^n_{Eq} - (\partial_x \eta)^n_{Eq} \right) . \tag{86}$$

Then we calculate the new η by the forward-in-time formula

$$\eta^{n+1}_{Eq} = \eta^n_{Eq} + \Delta t \, (\partial_t \eta)^n_{Eq} . \tag{87}$$

Next we consider the boundary condition for ϕ_j, (59). We use the following second-order central difference approximations for the second temporal and tangential derivatives [19]:

$$(\partial_t^2 \phi_{j-1})^n_{Eq} \simeq \frac{(\phi_{j-1})^{n+1}_{Eq} - 2(\phi_{j-1})^n_{Eq} + (\phi_{j-1})^{n-1}_{Eq}}{(\Delta t)^2} , \tag{88}$$

$$(\partial_y^2 \phi_{j-1})^{n+1}_{Eq} \simeq \frac{(\phi_{j-1})^{n+1}_{E,q+1} - 2(\phi_{j-1})^{n+1}_{Eq} + (\phi_{j-1})^{n+1}_{E,q-1}}{(\Delta y)^2} . \tag{89}$$

Note that (89) cannot be used at the two east corners (the two end points of Γ_E). At these corners, a one-sided second-order approximation should replace (89). For example, at the south-east corner we use [19]

$$(\partial_y^2 \phi_{j-1})^{n+1}_{Eq} \simeq \frac{2(\phi_{j-1})^{n+1}_{Eq} - 5(\phi_{j-1})^{n+1}_{E,q+1} + 4(\phi_{j-1})^{n+1}_{E,q+2} - (\phi_{j-1})^{n+1}_{E,q+3}}{(\Delta y)^2} . \tag{90}$$

From (59) we obtain a discrete formula for $\partial_t \phi_j$, i.e.,

$$(\partial_t \phi_j)^n_{Eq} \simeq \frac{1}{\beta_j} \left((\phi_{j+1})^n_{Eq} + \alpha_j (\partial_t^2 \phi_{j-1})^n_{Eq} + (\partial_y^2 \phi_{j-1})^{n+1}_{Eq} - \lambda (\phi_{j-1})^{n+1}_{Eq} \right) . \tag{91}$$

Then we calculate the new ϕ_j by the forward-in-time formula

$$(\phi_j)^{n+1}_{Eq} = (\phi_j)^n_{Eq} + \Delta t \, (\partial_t \phi_j)^n_{Eq} . \tag{92}$$

The simplest solution procedure is the one based on the sequential solution of the equations for the ϕ_j's. Namely, we first solve for η, then we solve for ϕ_1, then for ϕ_2, and so on. At the stage when we update the values of ϕ_j, the quantities $(\phi_{j-1})^{n+1}_{E\ldots}$

appearing in (88) and (89) are already known, having been derived in the previous stage for ϕ_{j-1}. On the other hand, the quantity $(\phi_{j+1})_{Eq}^{n+1}$ is not yet available; that is why we use $(\phi_{j+1})_{Eq}^{n}$ in (86) and (91) rather than $(\phi_{j+1})_{Eq}^{n+1}$. The latter fact may potentially lead to an unstable solution. Indeed, when we have implemented the scheme based on the formulas (85)–(92) with $J \geq 2$, an instability developed in time. A remedy for this instability is to perform a second iteration and update η and the ϕ_j's again based on values obtained in the first iteration. This two-cycle algorithm turns out to be stable. It is summarized in Box 2.

Note that the only algorithmic difference between the first and second iterations is in the use of $(\phi_1)_{Eq}^{n}$ vs. $(\phi_1)_{Eq}^{n+1}$ in (86). All the other formulas remain unchanged in the two iterations. We have tried to use also $(\phi_{j+1})_{Eq}^{n+1}$ in (91) instead of $(\phi_{j+1})_{Eq}^{n}$ in the second iteration, but this led to instability.

As an alternative scheme, eqs. (85)–(92) may be solved simultaneously for all the j's and all the y-locations q, as one coupled system of linear equations on Γ_E. The dimension of this system is JN_y, where N_y is the number of grid-points on Γ_E. In this case the part of the solution associated with the Higdon NRBC is implicit.

9. Controlling the Parameters

The Higdon NRBCs involve the parameters C_j which must be chosen. There are three approaches in this context:

(a) The user chooses the C_j a-priori in a manual manner based on an "educated guess." This is the procedure recommended in Higdon's papers [3]–[8].

(b) The C_j are chosen automatically by the computer code as a preprocess.

(c) The C_j are not constant, but are determined dynamically by the computer code. Namely, a value for C_j is estimated for every grid point on the boundary at each time step, from the solution in the previous time-steps.

We have adopted approach (b), which is automatic yet very inexpensive computationally. The algorithm we propose is described in Box 3. It is based on the *maximum resolvable* wave numbers in the x and y directions, and on the minimax formula [25] for choosing the x-component wave numbers. This algorithm seems to work well in practice and to yield reasonable estimates for the phase velocities.

The adaptive approach (c) is more complicated and costly. One possible scheme in this category is based on Fourier decomposition of the solution near the boundary Γ_E in each time step. Suppose an estimate of the C_j's is desired in a given time-step $n+1$ at a given point (x_E, y^*) on the boundary Γ_E. Then the proposed scheme consists of the following steps:

(1) Apply the one-dimensional Fast Fourier Transform (FFT) to the solution η^n along the boundary Γ_E. This will yield a number of Fourier modes in the y direction.

(2) Take an interval in the x direction going west from the point (x_E, y^*), namely an interval $x_{E-p^*} \leq x \leq x_E$, $y = y^*$, for some chosen integer p^*. Apply the

- *First iteration:*
- Compute the $(\partial_x \eta)^n$ values on Γ_E from (85).
- Compute the $(\partial_t \eta)^n$ values on Γ_E from (86).
- Compute the η^{n+1} values on Γ_E from (87).
- If $J = 1$, stop.
- For j=1,...,J-1:
  - Compute the $\partial_t^2(\phi_{j-1})^n$ values from (88).
  - Compute the $\partial_y^2(\phi_{j-1})^{n+1}$ values from (89) and (in the two corners) from (90).
  - Compute the $\partial_t(\phi_j)^n$ values from (91).
  - Compute the $(\phi_j)^{n+1}$ values from (92).
- Next j
- *Second iteration:*
- Recompute the $(\partial_t \eta)^n$ values on Γ_E from (86), but use $(\phi_1)^{n+1}$ instead of $(\phi_1)^n$.
- Recompute the η^{n+1} values on Γ_E from (87).
- For j=1,...,J-1:
  - Recompute the $\partial_t^2(\phi_{j-1})^n$ values from (88).
  - Recompute the $\partial_y^2(\phi_{j-1})^{n+1}$ values from (89) and (in the two corners) from (90).
  - Recompute the $\partial_t(\phi_j)^n$ values from (91).
  - Recompute the $(\phi_j)^{n+1}$ values from (92).
- Next j

Box 2. Algorithm for the FD implementation of the Jth-order Higdon NRBC based on the auxiliary-variable formulation.

- Given the grid parameter Δx, estimate the maximum resolvable wave number k in the x direction. Assuming a maximum of 10 grid points per wave length, a reasonable estimate is

$$k_{\max} = \frac{\pi}{5\Delta x} .$$

- Choose $J-1$ values of k from the interval $(0, k_{\max})$. This is done using the symmetric minimax formula (based on the Chebyshev polynomial) proposed by Sommeijer et al. [25]:

$$k_j = \left[\frac{k_{\max}^2}{2}\left(1+\cos\left(\frac{2j-1}{2(J-1)}\pi\right)\right)\right]^{\frac{1}{2}} , \qquad j = 1, \ldots, J-1 .$$

- Given the grid parameter Δy, estimate the maximum resolvable wave number k_y in the y direction. Again assuming a maximum of 10 grid points per wave length, a reasonable estimate is

$$(k_y)_{\max} = \frac{\pi}{5\Delta y} .$$

- For each k_j, calculate the corresponding (and maximal in the y direction) frequency ω_j from the dispersion relation (6):

$$\omega_j = \sqrt{C_0^2\left[k_j^2 + (k_y)_{\max}^2\right] + f^2} .$$

- Calculate

$$C_j = \frac{\omega_j}{k_j} \qquad \text{for} \quad j = 1, \ldots, J-1 .$$

- Add the value C_0 (the minimum possible phase speed) to the $J-1$ values calculated above. These constitute the desired J values C_j.

Box 3. Algorithm for determining the parameters C_j in the Higdon NRBC.

one-dimensional FFT to the solution η^n in this interval. This will yield a number of Fourier modes in the x direction.

(3) Take the products of the x- and y-Fourier coefficients obtained above. These products are the Fourier coefficients of the two-dimensional solution in the vicinity of the point (x_E, y^*). Among these 2D modes, pick the J modes which have the largest Fourier coefficient products.

(4) These J modes are associated with wave numbers $(k_x, k_y)_j$ for $j = 1, \ldots, J$. Extract the k_x's and k_y's from the appropriate one-dimensional modes.

(5) For each pair $(k_x, k_y)_j$, calculate the corresponding phase velocity $(C_x)_j$ (via the dispersion relation and (9)). These are the desired Higdon coefficients C_j.

It should be remarked that one does not necessarily have to use this procedure in every single time step and for every single grid point on Γ_E. In order to save in computations one may choose to use it more selectively.

10. A Numerical example

We apply the new scheme to a simple test problem whose exact solution is synthesized a priori. We consider the linear inhomogeneous Klein-Gordon equation,

$$\partial_t^2 u - C_0^2 \nabla^2 u + f^2 u = S \ , \tag{93}$$

in a two-dimensional uniform semi-infinite channel or wave guide. A Cartesian coordinate system (x, y) is introduced such that the wave-guide is parallel to the x direction. The width of the wave-guide is denoted b. We set $b = 5$, $C_0 = 1$ and $f = 0.5$. The boundary function $u_W(y, t)$ on Γ_W and the initial conditions are those that correspond to a solution $u(x, y, t)$ which is a linear combination of three waves of the form (5), i.e.,

$$u = \sum_{m=1}^{3} A_m \cos \frac{n_m \pi y}{b} \cos(k_m x - \omega_m t) \ . \tag{94}$$

The parameters chosen in (94) are:
$A_m = 1, \quad 1, \quad 1$;
$n_m = 1, \quad 2, \quad 2$;
$\omega_m = 0.81, \quad 1.37, \quad 1.68$.
This corresponds to the three phase velocities:
$C_x/C_0 = 7.61, \quad 6.27, \quad 1.69$.
The k_m in (94) are obtained from the ω_m and the n_m via the dispersion relation (6).

We introduce the artificial boundary Γ_E (see Fig. 1) at $x_E = 5$. Thus, the computational domain Ω is a 5×5 square. In Ω we use a uniform grid with 21×21 points. We discretize the Klein-Gordon equation in Ω using the explicit central-difference FD interior scheme (31). On Γ_E we impose the Higdon NRBC implemented in its high-order form. The time-step size is $\Delta t = 0.025$, which is smaller than the CFL limit and thus guarantees stability.

In Figs. 2(a)–(d), we plot the solution u at the point $x = 5$, $y = 2.75$ (located on Γ_E) as a function of time. In each of the four figures the exact solution is compared to a number of numerical solutions obtained with different NRBC schemes, namely with different choices of the order J and the parameters C_j. First we choose $C_j = 1$ for all j. Fig. 2(a) shows the H_1, H_2 and H_3 solutions. Their accuracy is poor, although the H_3 solution is significantly better than the other two. Fig. 2(b) shows the H_5 and H_7 solutions. The H_7 solution is quite accurate in the entire time interval shown. Thus, if the C_j's are not specially chosen, we need the order of the Higdon NRBC to be as high as 7 for high accuracy.

Now we employ the procedure given by Box 3 to automatically choose the C_j's. Fig. 2(c) shows the resulting H_3, H_4 and H_5 solutions. We see that in this case the approach of the numerical solutions to the exact solution is monotone. Moreover, for $J = 5$ we get about the same level of accuracy as we did with $J = 7$ when all the C_j had the value one (Fig. 2(b)). For additional reference, we show in Fig. 2(d) the H_3 solution obtained with the C_j corresponding to the three phase velocities C_x of the exact solution. It is about as accurate as the H_5 solution in Fig. 2(c). We also show the H_4 solution obtained with the exact C_1, C_2, C_3 and with $C_4 = 1$. The numerical solution is indistinguishable from the exact solution. In this case not only the NRBC is exact, but we gain additional accuracy on the boundary due to the increased order of the FD scheme.

This example demonstrates, albeit in a simplified setting, that the same level of accuracy obtained with parameter values C_j that are well-estimated can be achieved with ill-chosen parameter values but with an increased order J. Of course, increasing the order to ensure high accuracy is computationally expensive, and therefore it is usually beneficial to use the algorithm given in Box 3.

11. Nonzero Advection

When using the Higdon NRBC (4) with the SWEs, it has been assumed that the SWEs are linearized (at least in the exterior domain D) about the state of zero mean flow (no advection). Now, suppose that the SWEs are linearized about a state corresponding to a *nonzero* mean flow. For simplicity, let us assume that this mean flow is constant in space and time. If the component of the advection velocity in the x direction (the direction normal to Γ_E) is U_0, then in the non-dispersive case, the Sommerfeld-like condition $(\partial_t + C_0\partial_x)\eta = 0$ simply becomes $(\partial_t + (U_0 + C_0)\partial_x)\eta = 0$ (see, e.g., Durran [23]). We can infer from this, that the Higdon NRBCs (4) should be replaced by

$$H_J: \qquad \left[\prod_{j=1}^{J}\left(\partial_t + \hat{C}_j\partial_x\right)\right]\eta = 0 \quad \text{on} \quad \Gamma_E \qquad , \qquad \hat{C}_j = U_0 + C_j. \tag{95}$$

Thus, the Higdon conditions remain unchanged in the presence of advection, except that the parameter multiplying the x-derivative in each operator factor stands for the *total* phase velocity in the x direction (and not the perturbed velocity).

The high-order FD discretization scheme given in Section 3 above applies immedi-

ately to the advective case, with C_j replaced by $\hat{C}_j$. The interior scheme discussed in Section 5 and the scheme for selecting the parameters given in Section 9 can be extended to the advective case without difficulty. On the other hand, the discretization scheme devised in Section 6 (using auxiliary variables) cannot easily be adapted to the advective case, because it is inherently based on the linear Klein-Gordon equation (45). The latter is satisfied by η only in the non-advective case. In fact, it seems that with

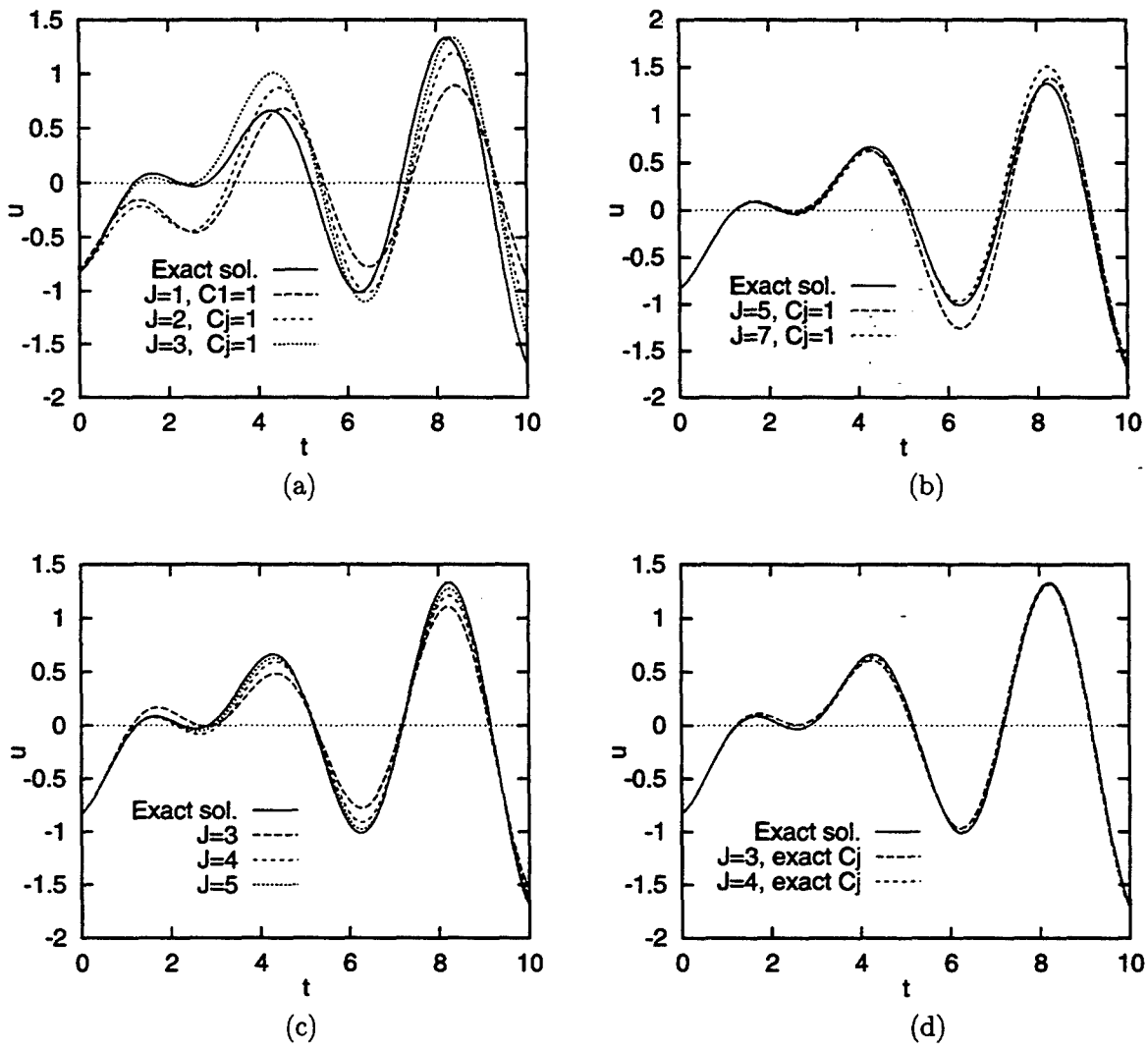

Figure 2: Solution of the three-wave test problem: u at the point $x = 5$, $y = 2.75$ (on Γ_E) as a function of time. (a) Exact solution and the H_1, H_2 and H_3 solutions with $C_j = 1$. (b) Exact solution and the H_5 and H_7 solutions with $C_j = 1$. (c) Exact solution and the H_3, H_4 and H_5 solutions with automatically chosen C_j. (d) Exact solution and the H_3 and H_4 solutions with the exact C_j.

nonzero mean flow, the linearized SWEs cannot be reduced to any single equation in η.

12. Blending the High-Order NRBCs with Global Data

In meteorology, one distinguishes between a Global Model (GM), in which the atmospheric equations are solved over the entire spherical surface of the globe, and a Limited-Area Model (LAM), in which the solution is sought in a relatively small region Ω bounded by artificial boundaries. The GM captures the large-scale atmospheric phenomena and is based on a coarse grid (about 100km resolution), whereas the LAM captures the mesoscale phenomena and is based on a finer grid (typically 10-20km resolution). The LAM is usually used after the solution of the GM is already available. One very important question in computational meteorology is: How should the information obtained from the GM be incorporated in the LAM? If we look at the east artificial boundary Γ_E of the LAM, for example, we face a dilemma: on one hand we wish to impose a NRBC on Γ_E, so that waves generated in Ω can leave the domain without spurious reflection, but on the other hand we wish to use the global data.

Three possible methods for blending global information with a NRBC are:

- One can use a "relaxation layer" for gradual transition from the LAM solution to the GM solution. One such scheme has been proposed in 1976 by Davies, and is still used today in the Navy code COAMPS [15] (where the global information is taken from the code NOGAPS).
- One can pose the whole LAM problem variationally (as is done when FE schemes are employed), use the NRBC on Γ_E, and apply the additional condition that the GM solution matches the LAM solution on Γ_E as a *constraint*. This constraint can be imposed by means of a Lagrange multiplier.
- One can extend an idea of Carpenter [27], which has been originally presented in the context of the Sommerfeld-like NRBC. Here is the basic idea. Suppose we have a NRBC of the form $H[\text{wave}] = 0$ on Γ_E, where H is a linear NRBC operator. We denote the solution obtained from the GM by u_G and the unknown solution of the LAM by u. We decompose both solutions into an *incoming* part and an *outgoing* part. We require the outgoing part of both solutions to satisfy the NRBC, and the incoming parts to match on Γ_E. Thus, we obtain the following five equations:

$$\text{Decomposition:} \quad u = u^{IN} + u^{OUT} \quad \text{on } \Gamma_E \tag{96}$$

$$\text{Decomposition:} \quad u_G = u_G^{IN} + u_G^{OUT} \quad \text{on } \Gamma_E \tag{97}$$

$$\text{Patching:} \quad u^{IN} = u_G^{IN} \quad \text{on } \Gamma_E \tag{98}$$

$$\text{NRBC:} \quad H[u^{OUT}] = 0 \quad \text{on } \Gamma_E \tag{99}$$

$$\text{NRBC:} \quad H[u_G^{OUT}] = 0 \quad \text{on } \Gamma_E \tag{100}$$

Using these five equation, one can obtain the single equation

$$H[u - u_G] = 0 \quad \text{on} \quad \Gamma_E \,. \tag{101}$$

Eq. (101) is a boundary condition which combines the chosen NRBC and the global information from the GM. This allows the use of any NRBC, including the Higdon high-order NRBCs, in the meteorology LAM.

13. Curved Artificial Boundaries

Since the shape of the artificial boundary $\mathcal{B}$ can be chosen by the code developer, it may seem that there is no particular need to work with non-rectangular boundaries. This is indeed the case in most applications of meteorology. However, in other fields, such as acoustics, there is a lot of interest in non-rectangular boundaries. Computational "boxes" have *corners* which sometimes give rise to numerical difficulties. Also, in exterior radiation or scattering problems it is more natural to think of the solution as composed of cylindrical or spherical waves (in the 2D and 3D cases, respectively) than of plane waves. For these reasons, it is of interest to develop high-order NRBC schemes in cylindrical and spherical coordinates, where the artificial boundary $\mathcal{B}$ is a circle and sphere, respectively. (Other curvilinear coordinates are also of interest in acoustics.)

It may be hard (or impossible) to generalize the auxiliary-variable scheme proposed in Section 6 to the cylindrical or spherical cases, because it relies heavily of the Cartesian structure of the wave equation. (The cylindrical case is actually more problematic; no converging high-order NRBCs are available today in 2D.) But the FD scheme presented in Section 3 *can* be generalized to both cases.

In 3D, with spherical coordinates, the NRBC analogous to the Higdon NRBC is

$$\left[\prod_{j=1}^{J} (\partial_t + C_j \partial_r)\right] (r^J \eta) = 0 \quad \text{on} \quad \mathcal{B} \,. \tag{102}$$

See a slightly more simplified condition in Bayliss and Turkel [28] (p. 710, eq. (2.3)). If one chooses $C_j = C_0$ for all the j's, and if there is no dispersion ($f = 0$), then (102) is exact for the first J spherical harmonics of the solution. It was shown by Neta that this condition is equivalent to

$$\sum_{i=0}^{J} \binom{J}{i} \frac{J!}{(J-i)!r^i} \prod_{k=1}^{J-i} (\partial_t + C_k \partial_r)\, \eta = 0. \tag{103}$$

In 2D, with polar coordinates, (102) is replaced by

$$\left[\prod_{j=1}^{J} (\partial_t + C_j \partial_r)\right] (r^{J-1/2} \eta) = 0 \quad \text{on} \quad \mathcal{B} \,. \tag{104}$$

In this case the NRBC is only *asymptotically* correct. It was shown by Neta that this condition is equivalent to

$$\sum_{i=0}^{J} \binom{J}{i} \frac{(2J-1)!!}{(2J-2i-1)!!(2r)^i} \prod_{k=1}^{J-i} (\partial_t + C_k \partial_r)\, \eta = 0. \tag{105}$$

Neta [29] has shown how to discretize (103) and (105) by FDs in a high-order way analogous to that shown in Section 3.

Acknowledgments

The first author would like to express his gratitude for the support extended to him by the National Research Council Associateship Programs. Both authors acknowledge the support from ONR (Marine Meteorology and Atmospheric Effects) grant N0001402WR20211 managed by Dr. Simon Chang and by the Naval Postgraduate School.

Appendix: Future Research

Here is the list of subjects for further investigation (in random order):

1. Thorough investigation of the numerical properties of the scheme: measuring the error as a function of the location of the artificial boundary; computing time and operation count as a function of the various parameters (such as J and the number of grid points on the boundary); stability with various interior schemes; etc.
2. Implementing the scheme with auxiliary variables, using FDs. (Being done now.)
3. Implementing the scheme with auxiliary variables using FEs. (Igor Patlashenko is working on this now.)
4. Experimenting with the use of the Higdon conditions with the Nonlinear SWEs in the computational domain. (Need to find a stable interior scheme-NRBC combination.)
5. Using the scheme with a rectangular artificial boundary (four non-reflecting edges). Checking if the corners are problematic. Also: applying the scheme in the 3D case.
6. Extending the scheme to the case of the linearized SWEs with a nonzero mean flow (advection).
7. Extending the scheme to the case of stratified media (say, a two-layers medium).
8. Blending the Higdon NRBCs with global information.
9. Updating the Higdon parameters C_j dynamically and adaptively. (May be needed in the stratified case, and nice to have as an option in all cases.)
10. Extending the scheme to curved boundaries. (May be not so important in meteorology, but certainly useful in acoustics.)

References

[1] J. Pedlosky, *Geophysical Fluid Dynamics*, Springer, New York, 1987.

[2] B. Gustafsson, H.-O. Kreiss and J. Oliger, *Time Dependent Problems and Difference Methods*, Wiley, New York, 1995.

[3] R.L. Higdon, "Radiation Boundary Conditions for Dispersive Waves," *SIAM J. Numer. Anal.*, **31**, 64–100, 1994.

[4] R.L. Higdon, "Absorbing Boundary Conditions for Difference Approximations to the Multi-Dimensional Wave Equation, *Math. Comput.*, **47**, 437–459, 1986.

[5] R.L. Higdon, "Numerical Absorbing Boundary Conditions for the Wave Equation," *Math. Comput.*, **49**, 65–90, 1987.

[6] R.L. Higdon, "Radiation Boundary Conditions for Elastic Wave Propagation," *SIAM J. Numer. Anal.*, **27**, 831–870, 1990.

[7] R.L. Higdon, "Absorbing Boundary Conditions for Elastic Waves," *Geophysics*, **56**, 231–241, 1991.

[8] R.L. Higdon, "Absorbing Boundary Conditions for Acoustic and Elastic Waves in Stratified Media," *J. Comput. Phys.*, **101**, 386–418, 1992.

[9] R.A. Pearson, "Consistent Boundary Conditions for the Numerical Models of Systems That Admit Dispersive Waves," *J. Atmos. Sci.*, **31**, 1418–1489, 1974.

[10] I. Orlanski, "A Simple Boundary Condition for Unbounded Hyperbolic Flows," *J. Comp. Phys.*, **21**, 251–269, 1976.

[11] W.H. Raymond and H.L. Kuo, "A Radiation Boundary Condition for Multi-Dimensional Flows," *Q.J.R. Meteorol. Soc.*, **110**, 535–551, 1984.

[12] M.J. Miller and A.J. Thorpe, "Radiation Conditions for the Lateral Boundaries of Limited-Area Numerical Models," *Q.J.R. Meteorol. Soc.*, **107**, 615–628, 1981.

[13] J.B. Klemp and D.K. Lilly, "Numerical Simulation of Hydrostatic Mountain Waves," *J. Atmos. Sci.*, **35**, 78–107, 1978.

[14] M. Wurtele, J. Paegle and A. Sielecki, "The Use of Open Boundary Conditions with the Storm-Surge Equations," *Mon. Weather Rev.*, **99**, 537–544, 1971.

[15] R.M. Hodur, "The Naval Research Laboratory's Coupled Ocean/Atmosphere Mesoscale Prediction System (COAMPS)," *Mon. Wea. Rev.*, **125**, 1414-1430, 1997.

[16] X. Ren, K.H. Wang and K.R. Jin, "Open Boundary Conditions for Obliquely Propagating Nonlinear Shallow-Water Waves in a Wave Channel," *Comput. & Fluids*, **26**, 269–278, 1997.

[17] T.G. Jensen, "Open Boundary Conditions in Stratified Ocean Models," *J. Marine Systems*, **16**, 297–322, 1998.

[18] F.S.B.F. Oliveira, "Improvement on Open Boundaries on a Time Dependent Numerical Model of Wave Propagation in the Nearshore Region," *Ocean Eng.*, **28**, 95–115, 2000.

[19] J.C. Tannehill, D.A. Anderson and R.H. Pletcher, *Computational Fluid Mechanics and Heat Transfer*, 2nd ed., Taylor & Francis, Washington DC, 1997.

[20] M.J. Miller and R.P. Pearce, "A Three Dimensional Primitive Equation Model of Cumulonimbus Convection, *Quart. J. Roy. Met. Soc.*, **100**, 133–154, 1974.

[21] J.C. Strikwerda, *Finite Difference Schemes and Partial Differential Equations*, Wadsworth & Brooks, Pacific Grove, CA, 1989.

[22] C.B. Vreugdenhil, *Numerical Methods for Shallow Water Flow*, Kluwer, Dordrecht, 1994.

[23] D.R. Durran, *Numerical Methods for Wave Equations in Geophysical Fluid Dynamics*, Springer, New York, 1999.

[24] T.J.R. Hughes, *The Finite Element Method*, Prentice-Hall, New Jersey, 1987.

[25] B.P. Sommeijer, P.J. van der Houwen and B. Neta, "Symmetric Linear Multistep Methods for Second-Order Differential Equations with Periodic Solutions," Report NM-R8501, Dept. of Numerical Mathematics, Center for Mathematics and Computer Science, Amsterdam, 1985. Also appeared in *Applied Numerical Mathematics*, **2**, 69–77, 1986.

[26] H.C. Davies, "A Lateral Boundary Formulation for Multi-Level Prediction Models," *Quart. J. R. Met. Soc.*, **102**, 405–418, 1976.

[27] K.M. Carpenter, Note on "Radiation Conditions for Lateral Boundaries of Limited-Area Numerical Models," by M.J. Miller and A.J. Thorpe, *Quart. J. R. Met. Soc.*, **108**, pp. 717–719, 1982.

[28] A. Bayliss and E. Turkel, "Radiation Boundary Conditions for Wave-Like Equations," *Comm. Pure Appl. Math.*, **33**, 707–725, 1980.

[29] B. Neta, Notes.

INITIAL DISTRIBUTION LIST

1.	Defense Technical Information Center 8725 John J. Kingman Rd., STE 0944 Ft. Belvoir, VA 22060-6218	2
2.	Dudley Knox Library, Code 013 Naval Postgraduate School Monterey, CA 93943-5100	2
3.	Research Office, Code 09 Naval Postgraduate School Monterey, CA 93943-5000	1
4.	Dan Givoli Naval Postgraduate School Department of Applied Mathematics Monterey, CA 93943	3
5.	Beny Neta, Code MA/Nd Naval Postgraduate School Department of Applied Mathematics Monterey, CA 93943	3
6.	Clyde Scandrett, Code MA/Sd Naval Postgraduate School Department of Applied Mathematics Monterey, CA 93943	1